- Electrochemical removal and recovery of phosphorus as
- struvite in an acidic environment using pure magnesium vs.

the AZ31 magnesium alloy as the anode

5 László Kékedy-Nagy^a, Ali Teymouri^b, Andrew M. Herring^b and Lauren F. Greenlee^a*

^a Ralph E. Martin Department of Chemical Engineering, University of Arkansas, 3202 Bell

Engineering Center, Fayetteville, AR 72701, United States

^b Department of Chemical and Biological Engineering, Colorado School of Mines, Golden, CO

9 80401, United States

*Corresponding author: Tel.: 610-507-6390, e-mail: greenlee@uark.edu

Abstract

4

6

7

8

10

11

12

13

14

15

16

17

18

19

20

Magnesium electrodes were investigated as the only source of magnesium for anodically-driven struvite precipitation in a single-cell electrochemical batch reactor. The cell was operated in an acidic environment with no pH adjustment. The effect of electrode composition on cell efficiency toward struvite production was investigated for pure Mg versus an AZ31 Mg alloy. In a 6 h batch experiment, the pure Mg anode out-performed the AZ31 alloy by producing a 4.5-fold greater mass of struvite and a 2.8-fold higher steady-state current density. The measured Mg dissolution rates were 1.2 mg cm⁻² h⁻¹ for the pure Mg and 0.8 mg cm⁻² h⁻¹ for the AZ31 Mg alloy anode, respectively. The structure, morphology, and composition of the electrochemically precipitated struvite were analyzed by x-ray

diffraction, scanning electron microscopy, x-ray photoelectron spectroscopy, and energy-dispersive x-ray spectroscopy. Results showed a crystalline struvite state, with an elongated needle-shaped morphology and a particle size of ca. 30 μm in length and ca. 6.5 μm in width. The smooth sharp edges are an indication of high-quality pure struvite, with no evidence of other precipitates or interfering cations.

Keywords. Electrochemical precipitation, Struvite, Magnesium sacrificial anode, Phosphorus recycling, Nutrient management

1. Introduction

Municipal and agricultural wastewater streams are characterized by a high level of organic matter, ammonia, and phosphorus content. This pollutant content leads to eutrophication of surface waters, and the effluents must, therefore, be treated before discharging the wastewater into receiving water bodies to reduce potential environmental impacts [1]. Most of the phosphate (ca. 2-20%) [2, 3] in wastewater ends up either in the wastewater sludge solids and subsequently disposed of in landfills or in the discharged effluent. Phosphate is, however, a limited mineral resource on Earth [4, 5], where 80-90% of phosphate is mined from rocks and its geographic concentration may lead to geopolitical tensions [6]. Thus, alternative sources of phosphorus should be considered, including recyclable and reusable sources from wastes (liquid or solid), to enable a sustainable global supply of phosphorus [7-9]. Importantly, it is estimated that ca. 20-22% of the world's consumption of phosphorus could be recovered by efficient wastewater treatment [3, 10, 11]. One potential approach to recover phosphates from wastewater, and other waste streams such as urine or manure, is by precipitation/crystallization of struvite [10, 12-16].

Struvite, magnesium ammonium phosphate hexahydrate (MgNH₄PO₄*6H₂O), is a poorly soluble mineral, comprised of stable white orthorhombic crystals that can deposit along the pipelines of wastewater and sewage sludge treatment plants [17, 18]. The general reaction for struvite precipitation can be expressed as follows:

48
$$Mg^{2+} + NH_4^+ + H_nPO_4^{n-3} + 6H_2O \rightarrow MgNH_4PO_4 * 6H_2O \downarrow + nH^+$$
 (1)

where n=0, 1 or 2 is based on the solution pH [14, 19]. Uncontrolled struvite formation in pipes and pumps is a well-recognized problem, and its consequences are numerous, all leading to a significant increase in the maintenance costs of a wastewater plant [20, 21]. Due to its chemical composition, struvite is also considered a premium grade, slow-release fertilizer, which is a potentially marketable product for the fertilizer industry and useable in agriculture [22]. For a controlled, large-scale struvite precipitation process to be successful and economically viable, the size of the recovered crystals must be controlled to prevent dissolution and to allow for effective particle separation. The purity is crucial for environmental reasons, where co-precipitation of heavy metals is undesirable in a fertilizer product and, where other precipitates (e.g., $Mg(OH)_2$) may decrease the efficacy for plant growth [19].

The development of struvite crystals follows two chemical stages: nucleation and crystal growth. Both stages are complex and controlled by several factors [23]. Commonly, the formation of struvite crystals is controlled by the concentration of Mg²⁺, NH₄⁺ and PO₄³⁻ ions, ionic strength, pH, temperature, mixing energy, and the presence of foreign ions [19, 24-27]. The pH is generally considered to be a key factor controlling struvite precipitation, as a result of the phosphate ions speciation, in other words, when the pH is increased the equilibrium is shifted toward PO₄³⁻ [13, 28]. Chemical precipitation is a widely used method for struvite production, where it has been shown that the optimal pH for high purity struvite is 7.5-9 [29]; however, the adjustment of pH required the

addition of uneconomic extra chemicals [20, 30-32]. Others have reported a lower optimal pH range 67 of 7-7.5 for the formation of pure struvite, although the precipitation rate of struvite was significantly 68 lower within this lower pH range [28]. 69 70 Electrochemical precipitation of struvite, where a sacrificial Mg alloy is used as the anode, eliminates 71 the need to add Mg from an external chemical source and potentially enables tunable control of pH 72 without chemical addition. In this approach, the necessary Mg for struvite precipitation is provided 73 from the anode as Mg ions due to corrosion. To our knowledge, Hug et al. [33] were the first to utilize this approach and precipitate struvite from source-separated urine, by using a Mg plate (type 74 MgAl3Zn1m%) as a sacrificial anode. The authors reported a phosphorus removal rate of 3.7 mg P 75 cm⁻² h⁻¹ at a current density of 55 A m⁻² [33]. Using the same concept and a high purity Mg alloy 76 (AZ91HP), Kruk et al. [31] achieved a slightly higher phosphorus removal rate of 4.0 mg P cm⁻² h⁻¹ 77 at a current density of 45 A m⁻². 78 79 The objectives of this study were to assess the feasibility of the electrochemical production of struvite from synthetic wastewater in an acidic environment and to compare the effect of two different types 80 of sacrificial anode compositions: pure-Mg vs. AZ31 magnesium alloy (Al 3 wt%, Zn 1 wt%, balance 81 Mg), as the only Mg source, on the overall struvite precipitation process, with the electrochemical 82 reactor setup described in Fig. 1. Precipitates on the surface of the anode, on the surface of the 83 cathode, and from the bulk solution were fully characterized for elemental composition, structure, 84 crystallinity, and morphology. To our knowledge, this work is the first of its kind to study the 85 production of struvite without any pH adjustment. 86

2. Materials and methods

2.1. Materials

87

Unless otherwise stated, all electrochemical experiments were performed with an aqueous solution containing $0.077~M~(7.53~g~L^{-1})$ ammonium dihydrogen phosphate (NH₄H₂PO₄) from Sigma-Aldrich. The test solutions were prepared by using Milli-Q water (18.2 M Ω , Millipore, Bedford, MA, USA). The magnesium foil (99.9% pure), AZ31 magnesium alloy foil and stainless-steel (316SS) plates of dimension 10~x~10~cm and 2 mm thick were purchased from Goodfellow Corporation. The flat plates later were cut in-house into four test electrodes of dimension 5~x~5~cm. The abrasive paper (Norton Abrasives) with different grain size used for polishing the electrodes was purchased at a local hardware store. The pH of the test solution was measured before and after the experiments by using a digital pH meter (Orion Star A111, Thermo Scientific). All batch experiments were carried out at room temperature, and each experiment with different anodes was repeated at least four times for reproducibility studies.

2.2. Reactor setup and electrolysis experiments

The electrolysis experiments were conducted in a single-compartment reactor filled with 0.85 L of 0.077 M test solution and continuously stirred at approximately 260 rpm. The schematic illustration of the reactor setup is given in Fig. 1, where the electrodes were shaped as thin plates with an active surface area of 40 cm² (NB: both sides of the electrodes were used). Pure-Mg or an AZ31 Mg alloy served as the anode, and 316SS served as the cathode, while the distance between the electrodes was held constant at 5 cm. The anode potential was controlled with a VSP-300 multichannel potentiostat/galvanostat (Bio-Logic, USA) and was measured against a double-junction Ag/AgCl (3M NaCl, BASi) reference electrode, where the reference electrode chamber was set close to the anode surface. Single batch experiments were conducted with each test lasting 6 h at a fixed anode potential of -0.8 V, proposed previously by others [33]. After each batch experiment, the precipitate from the anode and the cathode were collected and stored separately. The precipitate from the test solution was recovered by vacuum filtration, where the filter holder was fitted with PTFE un-laminated membrane

filters (0.45-micron, 47 mm from Sterlitech). The mass of the electrochemically precipitated struvite was determined with an analytical balance (Mettler Toledo, XSE105 Dual Range).

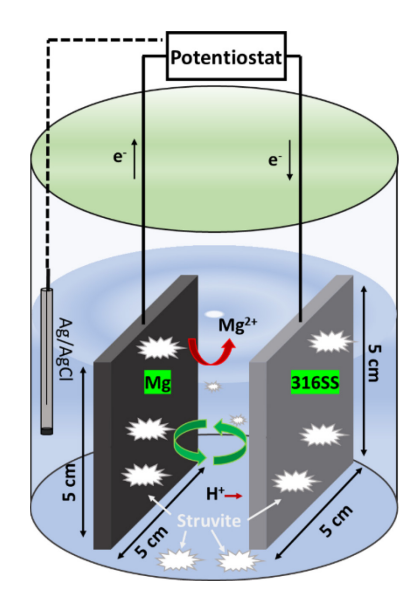


Fig. 1. Schematic illustration of the electrochemical setup, where a Mg anode was used as a sacrificial anode. In this setup, Mg was electrochemically dissolved and precipitated as struvite.

2.3. Surface and material characterization

The elemental composition and morphology of the electrochemically produced struvite were evaluated by using a scanning electron microscope (SEM) (FEI Nova Nanolab 200 Dual-Beam). The electrochemically obtained struvite crystal sizes were determined from the SEM images by using NIH Image/ ImageJ, an open source image-processing program. The crystal structure analysis was performed via x-ray diffraction (XRD) on a Philips PW1830 double system diffractometer equipped with a Cu cathode. X-ray photoelectron spectroscopy (XPS) data were obtained by using a PHI Versaprobe XPS scanning X-ray monochromator with a monochromatic Al K_{α} beam. Mg and P content in the precipitated solids and the electrolyte (solution) before and after the reaction were measured using the inductively coupled plasma–optical emission spectroscopy (ICP-OES)

(PerkinElmer Optima 8300) with a standard method 200.7 (US EPA, Rev. 4.4) to estimate the recovery of these elements in the overall process. The recovered solids were dissolved in 2.0 mL of 5 N nitric acid followed by the appropriate dilutions. All samples were filtered before the analysis using 0.2 μm nylon syringe filters (Fisherbrand, cat. no. 09-719-006). The ammonia concentration was measured with a high-range (0.4 – 50.0 mg/L NH₃-N) Hach standard kit using the salicylate method and a Hach DR 2800 spectrophotometer.

2.4. Calculations

125

126

127

128

129

130

131

The expected magnesium release from the anode based on the measured current ($m_{Mg,current}$) can be evaluated according to Faraday's law of electrolysis, and this current can be calculated by using the following equation [33]:

$$m_{Mg,\text{current}} = \frac{M_{Mg}Q}{zF}$$
 (2)

- where z is the magnesium valence (2), F is the Faraday constant (96485 C mol⁻¹), M_{Mg} is the molar mass of Mg (24.3 g mol⁻¹), and Q is the electric charge (C) obtained from the integration of the I vs. t curve (where I is current in A and t is time in s).
- Phosphorus removal efficiency as struvite using each of the two different anodes was calculated after the six-hour batch experiment using the following equation [34]:

141
$$P_{Rem} = \frac{(C_0 - C_t)}{C_0} \times 100\%$$
 (3)

- where P_{Rem} is the phosphorus removal efficiency (%), C_{θ} is the initial phosphorus concentration (mg L⁻¹), and C_t is the phosphorus concentration at time t (mg L⁻¹).
- The dissolution rate of the Mg during the batch experiments was determined according to the following equation [34]:

$$v_{Mg} = \frac{m_{Mg}}{(t \times A)} \tag{4}$$

where v_{Mg} is the rate of the total magnesium dissolved in the test solution (mg cm⁻² h⁻¹), m_{Mg} is the magnesium dissolved (mg), t is the time (h), and A is the active surface area of the specific anode (cm²).

3. Results and Discussion

3.1. Electrochemical struvite precipitation

To eliminate the effect of foreign ions and a possible co-precipitate alongside the struvite, the test solution contained only ammonium dihydrogen phosphate, and the pH of the test solution was not adjusted during the experiments. This synthetic wastewater composition allowed the fundamental study of the impact of the Mg anode composition on electrochemical struvite formation without any other complicating factors or parameters. While we recognize that this simplified system is far from a representative wastewater composition, our approach is based on the importance of understanding the behavior of the electrodes and the electrochemical system before proceeding to more complex water chemistries, particularly given the lack of prior literature on electrochemical struvite precipitation.

The initial pH of the test solution was 4.5 ± 0.1 and had increased to 6.0 ± 0.1 by the conclusion of each 6 h batch experiment. Thus, the experiments were carried out in an acidic environment. This measured range is below the optimum pH range considered for struvite precipitation and reported by others [31, 33, 35]. Based on the equilibrium between the three forms of the phosphate ion, the pH of the test solution is considered crucial for struvite precipitation: in alkaline solutions the PO₄³⁻ (HPO₄²⁻/PO₄³⁻ PK_a is ~ 12.67) [36-38] form dominates, whereas in weak acid solution the H₂PO₄- (H₃PO₄- (H₃PO

 pK_a is ~2.12) [36-38] form is more prevalent. In our system, the dominant form of phosphate is $H_2PO_4^-$, as the $H_2PO_4^-/HPO_4^{2-}$ pKa is ~7.21 [36-38].

Interestingly, when the anode and the cathode were placed in the test solution, at open circuit voltage (-1.6 V vs. Ag/AgCl, 3M NaCl), almost instantly, small fine particles were observed in the bulk solution. At the same time, a thin white passivation layer, most likely corresponding to struvite, was spotted on the surface of the electrodes. It is interesting to note that this phenomenon was also reported [35], but only when the solution pH was greater than 8.2. However, the study performed by Ben Moussa et al. [35] differs from the present study as the authors produced struvite by chemical precipitation and were interested in the critical pH corresponding to the spontaneous precipitation of struvite.

Chronoamperometric transients were recorded with the previously described electrochemical cell, and the results are shown in Fig. 2. The current density decreased slowly and reached a low steady value and we observed white crystals deposited on both the anode and the cathode. At the beginning of the experiments, higher current densities were measured for the AZ31 alloy compared to the pure-Mg (see Fig. 2, inset); however, the current density decrease of the AZ31 alloy was significantly greater over time. The formation of struvite on the anode produced a passivating layer that most likely inhibited the electron transfer between the electrodes and the test solution, which subsequently decreased the efficiency of the electrode for the electrochemically driven struvite precipitation. Based on these initial experiments, it appears that the passivating layer formed on the AZ31 alloy is far more detrimental to the effectiveness of the electrode compared to the pure-Mg anode. In other words, the properties of the precipitate layer formed on the AZ31 alloy reduce the ability of the alloy to corrode and release Mg ions, which reduces struvite formation.

It was shown previously [39] that the presence of Al and Zn ions (which are present in the composition of the AZ31 alloy) have an adverse effect on the crystal size of the struvite. Hutnik et al. [39] showed that the presence of Zn ions decreased the struvite crystal size by ca. 25%. It seems that this decrease in the crystal size produced a more compact film on the AZ31 alloy, which in turn had a more significant impact on the electrode fouling. In contrast, the struvite layer on the pure-Mg anodes, where there were no interfering ions present, presumably had larger crystals formed in their structure and produced a significantly less compact film; thus, the fouling was less significant.

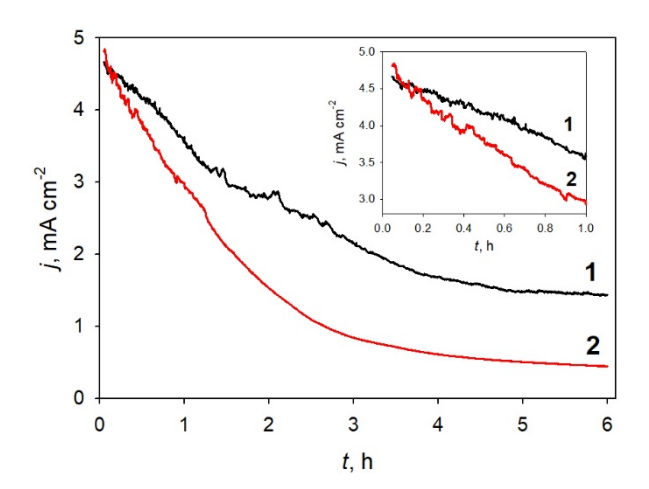


Fig. 2. The changes in the current density over time during the electrochemical precipitation of struvite on (1) pure-Mg and (2) AZ31 magnesium alloy anodes. Applied potential was -0.8 V vs. Ag/AgCl (3 M, NaCl). Inset: The change in the current density in the first hour using (1) pure-Mg and (2) AZ31 magnesium alloy anodes.

The steady state current density obtained for the pure Mg anode was 2.8-fold higher than that of the AZ31 alloy (Table 1). Furthermore, the theoretical Mg release ($m_{\text{Mg,current}}$), calculated according to Faraday's law of electrolysis, was 0.269 g for the pure Mg anode and 0.149 g for the alloy (Table 1). We note that our calculations do not account for any ohmic losses that may have occurred generally in the system and as a result of the passivating struvite precipitate layer on the surface of the anode

and cathode. This set of results suggests that the pure Mg anode likely produces a greater amount of struvite under the same test reaction conditions, as compared to the AZ31 alloy. The total weight of Mg that was released in each batch experiment in both the electrolyte and the precipitates was measured and compared by using ICP-OES analysis. In experiments where pure Mg was used as the anode, the total Mg released was 0.304 g, whereas for the AZ31 alloy, the total Mg released was 0.199 g. The observed higher Mg content in the precipitates and in the electrolyte after the 6 h batch experiments, as compared to the theoretical Mg release calculations, can be explained by the fact that the anodes might experience self-corrosion or loss of metal by spalling [31, 33, 40]. Song et al. [41] elegantly showed that the anodic dissolution of Mg in solutions containing phosphate or chloride is described by a heterogeneous electron transfer followed by a homogeneous chemical (EC) reaction. More specifically, in the first step Mg is electrochemically oxidized into an Mg⁺ intermediate (this step is assumed to be the rate-determining step), and in the second step, Mg⁺ is further oxidized to Mg^{2+} by the chemical H_2 evolution reaction. The pure Mg anode not only released a greater amount of magnesium but also produced a 4.5-fold greater amount of struvite over 6 h, as compared to the AZ31 alloy (Table 1). Thus, we conclude that the use of the pure-Mg is more beneficial towards efficient struvite production than the AZ31 alloy. The production of 1.8 g of struvite corresponds to a 11% yield for the pure-Mg, while the production of 0.4 g corresponds to a 3% yield for the AZ31 alloy, where the percent yield was determined from the expected struvite formation based on the known amount of ammonium and phosphate in the test solution. The expected struvite formation calculated from the measured current densities were 5.4 g (35%) for the pure Mg and 3.1 g (19%) for the AZ31 alloy, which are significantly higher compared to the obtained struvite in the batch experiments (Table 1).

201

202

203

204

205

206

207

208

209

210

211

212

213

214

215

216

217

218

219

220

221

222

At first glance, the low yields may be explained by the simple fact that we operated slightly under the optimum pH range considered for struvite precipitation, or by the sample collection method, where a significant amount may be lost (the struvite cannot be fully recovered from the anode surface due to pitting). In reality, the overall electrochemical struvite production process is quite complicated and involves multiple reactions occurring simultaneously at the electrode surface. At the anode surface, besides the formation of Mg²⁺ due to corrosion, H₂ and OH⁻ are also formed. The latter will increase the local pH, which in turn will shift the H₂PO₄⁻ toward HPO₄²- and PO₄³-. At the same time, at the cathode, surface water molecules are reduced to H₂ and OH⁻, produced by competing electrochemical reactions such as H₂ evolution reaction (HER). During the batch experiments, bubble formation on both the anode and the cathode was observed, which is evidence of the HER. Another competing reaction likely occurring on the cathode is the O₂ reduction reaction (ORR) which is typically a prevalent cathodic reaction on stainless steel [28, 31, 34]. Moreover, the formation of the insulating layer of struvite on the anode reduces the available surface area for active corrosion. All the abovementioned processes will influence the overall reaction yield of struvite. Further, in using Eq. (2) to calculate the estimated mass and yield of struvite from the current produced, we are assuming only Faradaic processes are the source of current produced, and we are ignoring non-Faradaic processes. However, non-Faradaic processes, including both ohmic losses and mass transport losses may occur. Ohmic losses are likely within the overall system and may also

224

225

226

227

228

229

230

231

232

233

234

235

236

237

238

239

240

241

242

243

244

245

246

247

produced, we are assuming only Faradaic processes are the source of current produced, and we are ignoring non-Faradaic processes. However, non-Faradaic processes, including both ohmic losses and mass transport losses may occur. Ohmic losses are likely within the overall system and may also increase during the electrochemical process as a result of formation of the passivating struvite layer on both the anode and the cathode. If ohmic and mass transport losses are significant in our system, our simple assumption of Faraday's law in our struvite calculations would lead to an over-estimate of Mg release and therefore an over-estimate of the theoretical struvite mass and yield expected, as predicted from the measured current. If we consider the values obtained for the mass and % yield of struvite predicted from the current produced ($m_{\text{struvite,current}}$ and Yield_{struvite,current}, Table 1) versus the

measured mass of struvite recovered (m_{struvite}), the larger values for the current-based predictions can be explained by an over-estimation as a result of excluding non-Faradaic losses in our calculations. Future work will include an effort to measure and account for ohmic losses within our electrochemical system and as a result of the struvite passivating layer on the electrode surfaces.

Table 1

Initial and final pH of the test solution, theoretical Mg release, the actual Mg release, current density, the amount of struvite and the yields obtained with the different anodes.

Anod	pH _i ^a	pH _f ^b	m _{Mg,current}	$m_{Mg}^{d}(\mathbf{g})$	j ^e	<i>m</i> struvite,curre	Yieldstruvitescurr	<i>m</i> _{struvit}	Yiel
e			° (g)		(mA	$_{\mathrm{nt}}{}^{\mathrm{f}}(\mathrm{g})$	ent ^g (%)	e h (g)	$\mathbf{d}^{\mathbf{i}}$
					cm ⁻²)				(%)
Pure-	4.6±0.	6.1±0.0	0.269±0.	0.304±0.	1.7±0.	5.4±1.1	35±7	1.8±0.	11±3
Mg	1	5	05	07	3			4	
AZ31	4.5±0.	5.9±0.0	0.149±0.	0.199±0.	0.6±0.	3.1±0.3	19±2	0.4±0.	3±0.
	1	6	02	05	2			1	8

^ainitial bulk pH; ^bfinal bulk pH; ^ctheoretical Mg release according to Eq. 2; ^dMg release determined by ICP-OES; ^esteady-state current density; ^famount of struvite expected from the measured current density; ^gpercent yield predicted from the measured current; ^hamount of struvite obtained after six-hour batch experiments; ⁱpercent yield of struvite obtained from the known amount of ammonium and phosphate in the solution.

3.2. Elemental characterization and nutrient recovery

Detailed characterization of the elemental composition (Mg:N:P) in precipitates recovered from the anode surface, the cathode surface, and the bulk solution are reported as molar ratios in Fig. 3. The data represent the average values of duplicate experiments and have a relative standard deviation (RSD) of less than 5%. The samples collected from the anode surface showed a Mg:N:P molar ratio

of 1.2:1:1 (pure-Mg) and 1.3:1:1 (AZ31). The molar ratios were comparable to the expected theoretical molar ratio of 1:1:1, which is considered the optimum for the high-grade purity struvite obtained by chemical precipitation [42, 43]. The higher Mg content, however, could be the result of the sample collection method (the precipitate is scraped off the anode surface). The samples collected from the cathode surface had the following molar ratios: 1:0.8:1 (pure-Mg) and 1.1:0.8:1 (AZ31), while the samples collected from the solution had 1.2:0.9:1 (pure-Mg) and 1.3:0.9:1 (AZ31), respectively. Although the phosphorus molar ratios recovered from the cathode surface and the bulk solution revealed to be slightly lower than that of anode, the differences are not statistically significant.

Elemental composition of the precipitates formed on the anode, cathode, and in the bulk solution as weight percentage (wt%) are illustrated in the Fig. A.1, where the reported values represent the average results from duplicate experiments and the error bars the standard deviation. The results show that the highest phosphorus removal occurred on the anode surface. Theoretically, the Mg, P, and N content of a pure struvite are 9.9, 12.6, and 5.7 wt%, respectively.

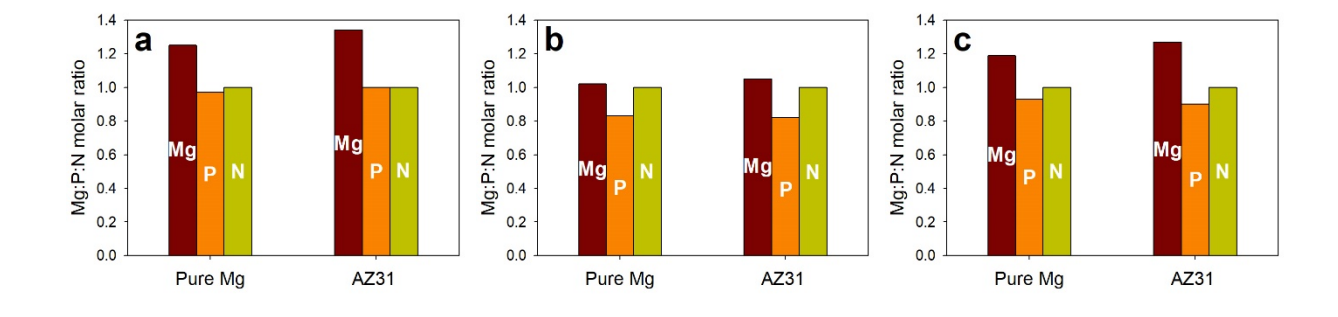


Fig. 3. The detailed characterization of the precipitated struvite on the (a) anode, (b) cathode, and (c) in the solution as molar percentage of the struvite (NB: the Mg:N:P molar ratios of high-grade purity struvite are 1:1:1).

Results from ICP-OES analysis performed on the solutions collected from the reactor after each 6-hour experiment are illustrated in Table 2. The results reveal that experiments conducted with AZ31 alloy as the anode have higher Mg and P concentrations remaining in solution (Table 2). The presence of Al and Zn in small concentrations in the test solution in the case of the AZ31 anode is the result of the alloy composition. These impurities were collected in the test solution during the corrosion process of the anode.

Table 2

Concentrations of elements presented in the solution after the experiments performed with pure magnesium and AZ31 alloy as the anode, performed by ICP-OES analysis.

Anode	Mg (ppm)	P (ppm)	Al (ppm)	Zn (ppm)
Pure-Mg	125±9.1	1453±118	0.0 ± 0.0	0.0±0.0
AZ31	146±5.1	1631±18.3	0.1±0.0	0.1±0.0

Studies performed with the pure Mg anode resulted in a lower P content in the remaining solution, which indicates a higher overall P recovery, see Table 2. Based on Eq. (3), the P and N removal efficiencies for the experiments conducted with pure Mg anode were 38.8±6.8 *wt*% and 16.0±5.8 *wt*%, respectively, compared to that of 31.6±0.5 *wt*% and 7.7±0.9 *wt*%, respectively, in the case of the AZ31 alloy. The overall Mg dissolution rates calculated according to Eq. (4) were 1.2 mg cm⁻² h⁻¹ for the pure-Mg and 0.8 mg cm⁻² h⁻¹ for the AZ31 Mg alloy anode, respectively. The higher dissolution rates obtained for the pure Mg anodes substantiates the higher total magnesium release determined with ICP-OES analysis.

3.3. Struvite analysis

297

298

299

300

301

302

303

304

305

306

307

308

309

310

311

312

313

314

315

316

317

318

319

320

Inspection after the 6 h batch experiments revealed that both the anode and the cathode were covered by struvite particles. Struvite precipitate was also observed in the test solution as well. To characterize the struvite from each of these sources, the struvite from both electrodes was carefully scraped off, while the struvite from the test solution was recovered by vacuum filtration. Next, the electrochemically obtained struvite was studied in detail by various surface characterization techniques. We note that our filtration recovery approach does not include any dissolved, solubilized struvite that may have remained in the saturated aqueous solution in our overall measurement of struvite recovery. While our measurements of the filtered solid struvite particles inherently miss accounting for the solubilized portion, we note that in a real struvite recovery process, only formed particulates would be easily recovered. Thus, our approach of focusing on the particulate struvite as the recoverable portion is relevant to an envisioned engineered wastewater treatment process, and with this approach, we are not over-estimating the possible struvite able to be recovered by also including a solubilized struvite contribution. The morphology of the precipitated crystals was characterized by XRD, and the results are presented in Fig. 4. The XRD patterns obtained from the electrochemically produced struvite were compared to the spectrum of struvite standard (PDF card no. 01-077-2303, Fig. A.2) and the commercially available struvite (Crystal Green) produced by chemical precipitation. The XRD patterns demonstrated high similarity in the peak position and intensity to both pure struvite (Fig. A.2) and the commercially available struvite. The difference in the peak intensities observed in the XRD patterns means that the structure of the precipitate might be different from that of the commercially available struvite. There were no additional diffraction peaks detected, which would correspond to another mineral, such as magnesium ammonium phosphate monohydrate, also known as dittmarite or magnesium phosphate [44, 45].

The surface morphology was further analyzed with XPS, where the spectra was obtained over the energy range of 0-1200 eV and 0-1400 eV (Fig. A.3-A.6). The electrochemically obtained struvite showed a high degree of similarity with XPS data reported previously [46] and compared to the commercially available struvite (Crystal Green). The core level peaks were Mg 1s (1303.7 eV), Mg 2p (50.2 eV), O 1s (532.6 eV), N 1s (400.1 eV), C 1s (282.5 eV) and P 2p (135.1 eV). It is worth mentioning that in the case of the AZ31 alloy, peaks corresponding to Ca can be observed, which are present in the alloy composition (0.040%).

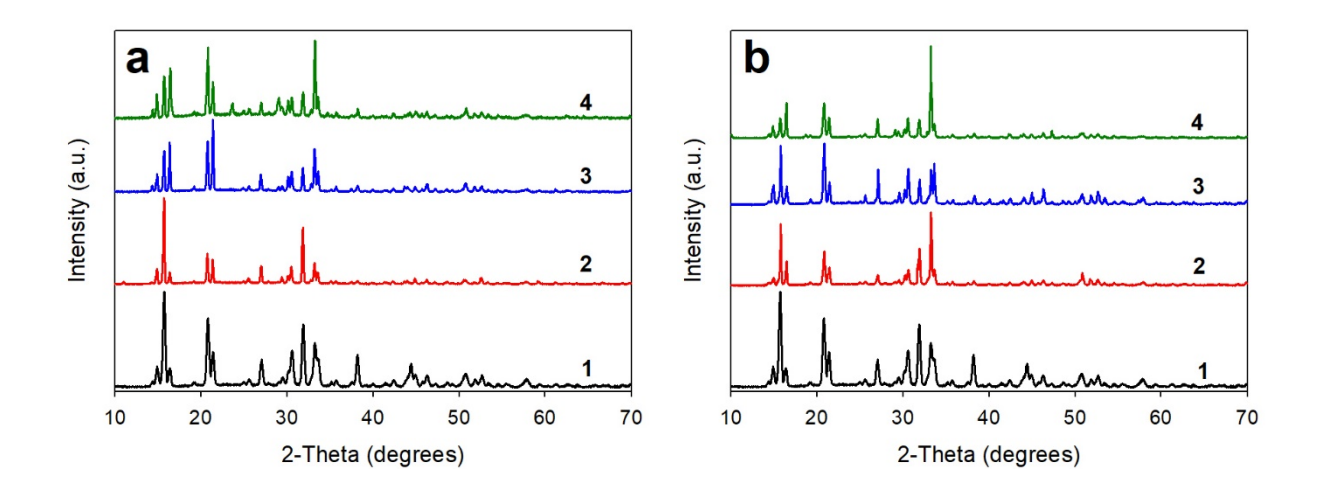


Fig. 4. XRD patterns of the (1) commercially available struvite (Crystal Green) and the electrochemically obtained struvite collected from (2) anode, (3) cathode, (4) bulk solution, where (a) pure Mg- and (b) AZ31 alloy was used as the anode, respectively.

The electrochemically obtained struvite crystals were also studied and analyzed by SEM, and results are shown in Fig. 5. In all cases, the crystals displayed an elongated, needle-shaped pattern with smooth, sharp edges, which is typical for high purity struvite [14, 19, 28, 47] and a particle size of ca. 30 µm in length, as well as, ca. 6.5 µm in width. The sharp, smooth edges suggested that there were no divalent cations present, which might affect the struvite crystal structure [19]. In the SEM images of struvite collected from the different anodes and cathode, respectively, smaller irregular shaped

crystals can be observed as well (Fig. A.7). These smaller crystal structures are most probably the result of the collection process, and it seems that certain crystals were damaged.

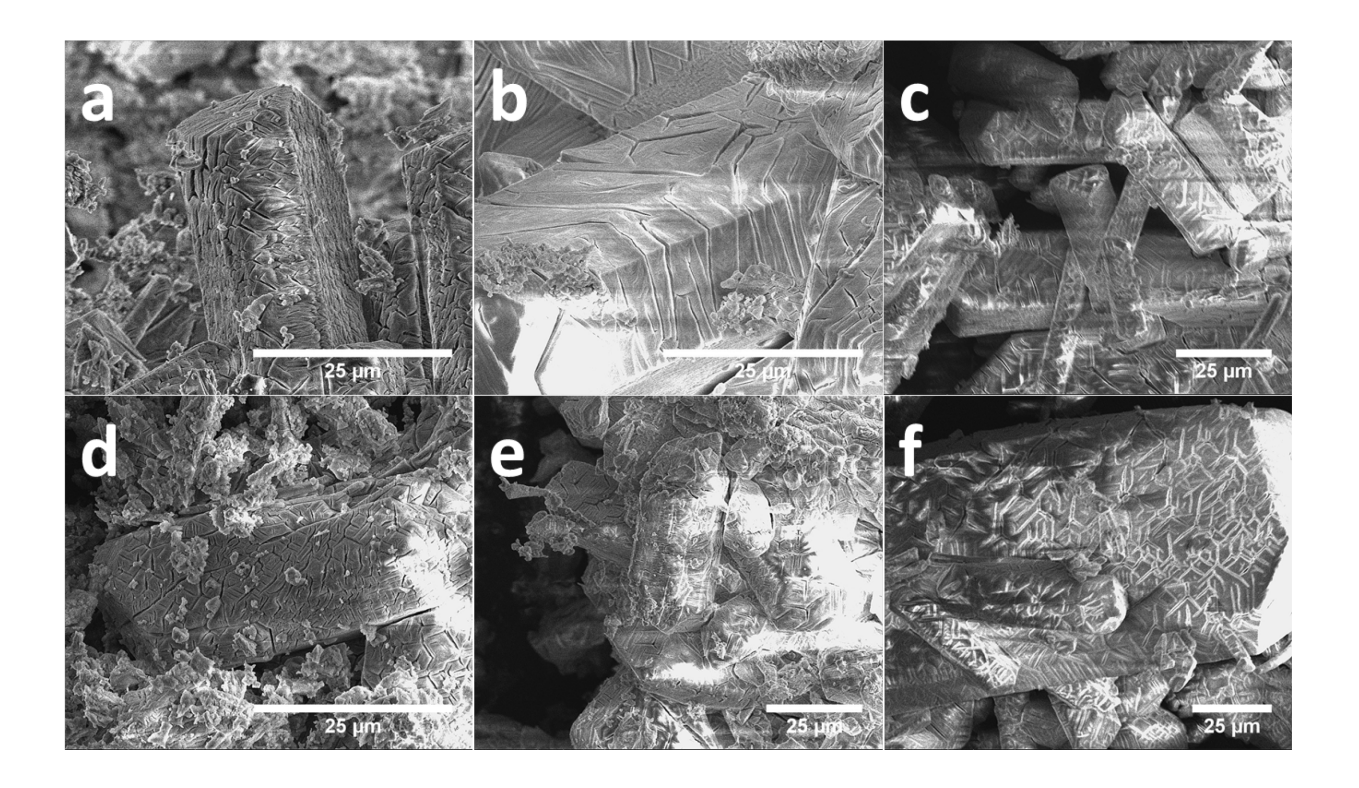


Fig. 5. SEM images of the electrochemically obtained struvite crystals after 6 h batch experiments, where pure-Mg (top) was used as anode and collected from (a) anode, (b) cathode, (c) test solution; and AZ-31 alloy (bottom) was used as anode and acquired from (d) anode, (e) cathode, and (f) test solution.

The EDX spectrums (Fig. A.8) showed that highest peaks were obtained for Mg, P, and O (major elements composing struvite in mass percentage), confirming the purity of the crystal formed. In the case when pure Mg was used as the anode, as expected, no traces of other compounds have been found in the struvite, regardless from where the sample was collected from (anode, cathode or the test solution, Fig. A.8). In the case of the AZ31 alloy, the EDX spectrum of the struvite recovered from the anode surface showed trace elements of Al and Zn, see Fig. A.9. Both metals are present in the AZ31 alloy, and their presence in the struvite can be explained by the fact that the samples were

collected by scraping them off from the anode surface. The samples collected from the cathode or the test solution did not contain any other elements in their EDX spectrum.

4. Conclusions

In summary, we showed the feasibility of electrochemical struvite precipitation with a simple reactor setup in acidic aqueous solutions, without pH adjustment, containing only ammonium dihydrogen phosphate and using a Mg sacrificial anode as the only source of Mg. We studied the effect of two different types of sacrificial anodes on struvite production: pure Mg vs. an AZ31 Mg alloy, where the reactor with the pure Mg anode outperformed the one with the AZ31 Mg alloy, by producing a 4.5-fold greater amount of struvite. In addition, the purity of the electrochemically precipitated struvite was determined with various surface characterization techniques, and they showed characteristics comparable to the commercially available and to the high-grade purity struvite standard. Overall, in this electrochemical reactor setup, the pure Mg anode showed a better performance towards the electrochemical struvite precipitation. On the other hand, further explorations on optimizing the reactor setup should be achieved in order to improve the percent yield of the system and to become a viable option in large-scale struvite production.

359 Acknowledgments

All of the authors acknowledge the National Science Foundation (NSF) for financial support of this work through the INFEWS/T3 Award #1739473 and the university of Arkansas Institute for Nanoscience and Nanotechnology characterization facility for support in surface and material characterization.

References

- 366 [1] L.E. De-Bashan, Y. Bashan, Recent advances in removing phosphorus from wastewater and its
- 367 future use as fertilizer (1997–2003), Water Res 38 (2004) 4222-4246.
- 368 [2] M.J. McLaughlin, Land application of sewage sludge: Phosphorus considerations, S Afr J Plant
- 369 Soil 1 (1984) 21-29.
- 370 [3] Z. Yuan, S. Pratt, D.J. Batstone, Phosphorus recovery from wastewater through microbial
- 371 processes, Curr. Opin. Biotechnol. 23 (2012) 878-883.
- 372 [4] O. Ichihashi, K. Hirooka, Removal and recovery of phosphorus as struvite from swine
- wastewater using microbial fuel cell, Bioresour. Technol. 114 (2012) 303-307.
- [5] J. Driver, D. Lijmbach, I. Steen, Why recover phosphorus for recycling, and how?, Environ.
- 375 Technol. 20 (1999) 651-662.
- 376 [6] N. Ma, A.A. Rouff, Influence of pH and oxidation state on the interaction of arsenic with
- 377 struvite during mineral formation, Environ. Sci. Technol. 46 (2012) 8791-8798.
- 378 [7] P. Ledezma, P. Kuntke, C.J.N. Buisman, J. Keller, S. Freguia, Source-separated urine opens
- 379 golden opportunities for microbial electrochemical technologies, Trends Biotechnol. 33 (2015) 214-
- 380 220.
- 381 [8] S. Kataki, H. West, M. Clarke, D.C. Baruah, Phosphorus recovery as struvite: Recent concerns
- for use of seed, alternative Mg source, nitrogen conservation and fertilizer potential, Resour
- 383 Conserv Recycl 107 (2016) 142-156.
- 384 [9] D. Cordell, A. Rosemarin, J.J. Schröder, A.L. Smit, Towards global phosphorus security: A
- systems framework for phosphorus recovery and reuse options, Chemosphere 84 (2011) 747-758.
- [10] C.A. Cid, J.T. Jasper, M.R. Hoffmann, Phosphate Recovery from Human Waste via the
- Formation of Hydroxyapatite during Electrochemical Wastewater Treatment, ACS Sustainable
- 388 Chem. Eng. 6 (2018) 3135-3142.

- 389 [11] J.R. Mihelcic, L.M. Fry, R. Shaw, Global potential of phosphorus recovery from human urine
- and feces, Chemosphere 84 (2011) 832-839.
- 391 [12] M. Ronteltap, M. Maurer, W. Gujer, Struvite precipitation thermodynamics in source-separated
- 392 urine, Water Res 41 (2007) 977-984.
- 393 [13] R.D. Cusick, B.E. Logan, Phosphate recovery as struvite within a single chamber microbial
- 394 electrolysis cell, Bioresour. Technol. 107 (2012) 110-115.
- 395 [14] M.P. Huchzermeier, W. Tao, Overcoming challenges to struvite recovery from anaerobically
- digested dairy manure, Water Environ. Res. 84 (2012) 34-41.
- 397 [15] H. Huang, D. Xiao, J. Liu, L. Hou, L. Ding, Recovery and removal of nutrients from swine
- wastewater by using a novel integrated reactor for struvite decomposition and recycling, Sci. Rep. 5
- 399 (2015) 10183.
- 400 [16] B. Li, I. Boiarkina, W. Yu, H.M. Huang, T. Munir, G.Q. Wang, B.R. Young, Phosphorous
- recovery through struvite crystallization: challenges for future design, Sci. Total Environ. (2018).
- 402 [17] M. Quintana, E. Sanchez, M.F. Colmenarejo, J. Barrera, G. Garcia, R. Borja, Kinetics of
- 403 phosphorus removal and struvite formation by the utilization of by-product of magnesium oxide
- 404 production, Chem. Eng. J. 111 (2005) 45-52.
- 405 [18] H. Saidou, S. Ben Moussa, M. Ben Amor, Influence of airflow rate and substrate nature on
- heterogeneous struvite precipitation, Environ. Technol. 30 (2009) 75-83.
- 407 [19] K.S. Le Corre, E. Valsami-Jones, P. Hobbs, S.A. Parsons, Impact of calcium on struvite crystal
- 408 size, shape and purity, J. Cryst. Growth 283 (2005) 514-522.
- 409 [20] J.D. Doyle, K. Oldring, J. Churchley, S.A. Parsons, Struvite formation and the fouling
- propensity of different materials, Water Res 36 (2002) 3971-3978.

- 411 [21] K.S. Le Corre, E. Valsami-Jones, P. Hobbs, S.A. Parsons, Phosphorus recovery from
- wastewater by struvite crystallization: A review, Crit. Rev. Environ. Sci. Technol. 39 (2009) 433-
- 413 477.
- 414 [22] J.A. Wilsenach, C.A.H. Schuurbiers, M.C.M. Van Loosdrecht, Phosphate and potassium
- recovery from source separated urine through struvite precipitation, Water Res 41 (2007) 458-466.
- 416 [23] M.L. Harrison, M.R. Johns, E.T. White, C.M. Mehta, Growth rate kinetics for struvite
- 417 crystallization, Chem. Eng. Trans 25 (2011) 309-314.
- 418 [24] C.M. Mehta, D.J. Batstone, Nucleation and growth kinetics of struvite crystallization, Water
- 419 Res 47 (2013) 2890-2900.
- 420 [25] S. Agrawal, J.S. Guest, R.D. Cusick, Elucidating the impacts of initial supersaturation and seed
- 421 crystal loading on struvite precipitation kinetics, fines production, and crystal growth, Water Res
- 422 132 (2018) 252-259.
- 423 [26] D. Kim, H.-D. Ryu, M.-S. Kim, J. Kim, S.-I. Lee, Enhancing struvite precipitation potential for
- ammonia nitrogen removal in municipal landfill leachate, J. Hazard. Mater. 146 (2007) 81-85.
- 425 [27] P. Battistoni, G. Fava, P. Pavan, A. Musacco, F. Cecchi, Phosphate removal in anaerobic
- liquors by struvite crystallization without addition of chemicals: preliminary results, Water Res 31
- 427 (1997) 2925-2929.
- 428 [28] C.-C. Wang, X.-D. Hao, G.-S. Guo, M.C.M. Van Loosdrecht, Formation of pure struvite at
- neutral pH by electrochemical deposition, Chem. Eng. J. 159 (2010) 280-283.
- 430 [29] A.N. Kofina, P.G. Koutsoukos, Spontaneous precipitation of struvite from synthetic
- wastewater solutions, Cryst. Growth Des. 5 (2005) 489-496.
- 432 [30] Y. Jaffer, T.A. Clark, P. Pearce, S.A. Parsons, Potential phosphorus recovery by struvite
- 433 formation, Water Res 36 (2002) 1834-1842.

- 434 [31] D.J. Kruk, M. Elektorowicz, J.A. Oleszkiewicz, Struvite precipitation and phosphorus removal
- using magnesium sacrificial anode, Chemosphere 101 (2014) 28-33.
- 436 [32] N.C. Bouropoulos, P.G. Koutsoukos, Spontaneous precipitation of struvite from aqueous
- 437 solutions, J. Cryst. Growth. 213 (2000) 381-388.
- 438 [33] A. Hug, K.M. Udert, Struvite precipitation from urine with electrochemical magnesium
- dosage, Water Res 47 (2013) 289-299.
- 440 [34] X. Lin, Z. Han, H. Yu, Z. Ye, S. Zhu, J. Zhu, Struvite precipitation from biogas digestion
- slurry using a two-chamber electrolysis cell with a magnesium anode, J. Clean. Prod. 174 (2018)
- 442 1598-1607.
- 443 [35] S. Ben Moussa, G. Maurin, C. Gabrielli, M.B. Amor, Electrochemical precipitation of struvite,
- Electrochem. Solid State Lett. 9 (2006) C97-C101.
- 445 [36] V.S. Stoll, J.S. Blanchard, [4] Buffers: Principles and practice, Methods in enzymology,
- 446 Elsevier1990, pp. 24-38.
- 447 [37] J. Yan, G. Springsteen, S. Deeter, B. Wang, The relationship among pKa, pH, and binding
- constants in the interactions between boronic acids and diols—it is not as simple as it appears,
- 449 Tetrahedron 60 (2004) 11205-11209.
- 450 [38] A. Krężel, W. Bal, A formula for correlating pKa values determined in D2O and H2O, J. Inorg.
- 451 Biochem 98 (2004) 161-166.
- 452 [39] N. Hutnik, A. Kozik, A. Mazienczuk, K. Piotrowski, B. Wierzbowska, A. Matynia, Phosphates
- (V) recovery from phosphorus mineral fertilizers industry wastewater by continuous struvite
- reaction crystallization process, Water Res 47 (2013) 3635-3643.
- 455 [40] G. Song, A. Atrens, Understanding magnesium corrosion—a framework for improved alloy
- 456 performance, Adv. Eng. Mater. 5 (2003) 837-858.

- 457 [41] G.L. Song, A. Atrens, Corrosion mechanisms of magnesium alloys, Adv. Eng. Mater. 1 (1999)
- 458 11-33.
- 459 [42] N.O. Nelson, R.L. Mikkelsen, D.L. Hesterberg, Struvite precipitation in anaerobic swine
- lagoon liquid: effect of pH and Mg: P ratio and determination of rate constant, Bioresour. Technol.
- 461 89 (2003) 229-236.
- 462 [43] J.R. Buchanan, C.R. Mote, R.B. Robinson, Thermodynamics of struvite formation, Trans.
- 463 ASAE 37 (1994) 617-621.
- 464 [44] M.I.H. Bhuiyan, D.S. Mavinic, F.A. Koch, Thermal decomposition of struvite and its phase
- transition, Chemosphere 70 (2008) 1347-1356.
- 466 [45] K.Z. Chong, T.S. Shih, Conversion-coating treatment for magnesium alloys by a
- permanganate-phosphate solution, Mater. Chem. Phys. 80 (2003) 191-200.
- 468 [46] H. Li, Q.-Z. Yao, S.-H. Yu, Y.-R. Huang, X.-D. Chen, S.-Q. Fu, G.-T. Zhou, Bacterially
- mediated morphogenesis of struvite and its implication for phosphorus recovery, Am. Mineral 102
- 470 (2017) 381-390.

- 471 [47] S. Graeser, W. Postl, H.-P. Bojar, P. Berlepsch, T. Armbruster, T. Raber, K. Ettinger, F.
- Walter, Struvite-(K), KMgPO4· 6H2O, the potassium equivalent of struvite-a new mineral, Eur J
- 473 Mineral 20 (2008) 629-633.